Original Article

Swept-source optical coherence tomography features of regressed macular retinoblastoma

Sourav Damodaran, Mandeep S Bajaj, Pradeep Sharma, Atul Kumar, Rohan Chawla, Amar Pujari, Gaurav Garg, Shreyas Temkar

Purpose: To describe the swept-source optical coherence tomography (SS-OCT) features of regressed macular retinoblastoma (RB). **Methods:** A cross-sectional observational study was carried out in 13 patients with regressed macular RB with good fixation in at least one eye. Fundus photography and SS-OCT were documented. High-resolution scans with good signal strength were selected. The types of clinical regression and SS-OCT characteristics of the regressed lesions (presence of vitreous detachment, intratumor schisis/cavitation, calcification, foveal dip, and OCT pattern) were noted. **Results:** Of the 13 eyes, 7 (53%) were group B, 4 (30%) were group C, and 2 (17%) were group D. Lesion involving fovea was seen in seven eyes (53%). On SS-OCT, the lesion was isodense to hyperdense in all cases. Three patterns of regressed RB were noted on OCT. Intralesion calcification was noted in eight cases. Subretinal fluid was not detected in any of the cases. **Conclusion:** SS-OCT is a useful technology to image and analyze cases of regressed macular RB including large lesions. SS-OCT system helps in successful imaging even in smaller children.

Key words: Optical coherence tomography, ocular tumors, retcam, retinal imaging, retinoblastoma

Access this article online

Website: www.ijo.in

DOI: 10.4103/ijo.IJO_533_19

Quick Response Code:

Retinoblastoma (RB) is the most common intraocular malignancy in children.[1,2] Recent advances in management have led to improved survival of children affected with RB with a 5-year cumulative survival rate of greater than 90%.[3,4] As the rate of globe salvage in RB cases has increased, the focus has shifted towards tumor monitoring using various imaging modalities.[5]

Various authors have described the utility of optical coherence tomography (OCT) in the management of different pediatric vitreoretinal disorders. Hand-held spectral-domain OCT (SD-OCT) has been shown to be an useful tool in conditions such as shaken baby syndrome, retinopathy of prematurity, and ocular albinism.[6-8] OCT is also being increasingly used in imaging patients with RB to look for tumor characteristics, monitor therapeutic response, identify recurrence, and to look for ophthalmoscopically invisible lesions.[9-12] A majority of these studies have been done using hand-held SD-OCT under general anesthesia. However, SD-OCT has limitations and is not useful for imaging large lesions due to limited depth of penetration.[13] The development of swept-source-OCT (SS-OCT) has resulted in rapid image acquisition and improved axial resolution (to the order of 1 μm). SS-OCT is an extremely useful tool for imaging choroid and it can even be used for imaging in cases with hazy media. In this study, we assess the utility of SS-OCT in cases of RB and describe the OCT patterns of regressed macular RB.

Methods

This was a cross-sectional observational study conducted at the Ocular Oncology and Retina Services of Dr. Rajendra Prasad Centre for Ophthalmic Sciences, All India Institute of Medical Sciences, New Delhi. The study adhered to the tenets of Declaration of Helsinki. Institute ethics committee clearance was taken prior to the beginning of study. The definition of macular RB was based on the definition given by Shields *et al*.[14] It was defined as tumor, any part of which is within 2DD (3 mm) of the center of macula. Regression was based on the clinical appearance of the tumor after successful response to various modalities of therapy. Only lesions of macular region were taken to facilitate ease of scanning and to avoid artifacts. Children with regressed macular RB in one or both eyes (but presence of good fixation in either of the eyes) were included in the study. Children who were not able to cooperate for the procedure were excluded. Detailed consent was obtained as per the institute protocol. Demographic data such as current age, age at diagnosis, gender, and laterality were noted. Previous treatment history was also noted with respect to the modalities of treatment (chemotherapy and local therapy) and time to regression. The clinical regression patterns were classified as type 0 (no visible residua), type 1 (fully or almost fully calcific residua), type 2 (fleshy

Dr. Rajendra Prasad Centre for Ophthalmic Sciences, All India Institute of Medical Sciences, New Delhi, India

Correspondence to: Dr. Shreyas Temkar, Dr. Rajendra Prasad Centre for Ophthalmic Sciences, All India Institute of Medical Sciences, Ansari Nagar, New Delhi - 110 029, India. E-mail: shreyastemkar@gmail.com

Received: 01-Apr-2019 Revision: 23-Jun-2019
Accepted: 08-Aug-2019 Published: 22-Nov-2019

Cite this article as: Damodaran S, Bajaj MS, Sharma P, Kumar A, Chawla R, Pujari A, *et al*. Swept-source optical coherence tomography features of regressed macular retinoblastoma. Indian J Ophthalmol 2019;67:2013-8.

tissue with little or no calcification), type 3 (mixed calcific and fleshy), and type 4 (atrophic chorioretinal flat scar).[15] Fundus photography was done using Retcam 3 (Clarity Medical Systems, USA) during examination under anesthesia or on regular fundus cameras (Triton DRI-OCT fundus camera; Topcon Corporation, Tokyo, Japan). SS-OCT was done on Triton DRI-OCT. Children were explained regarding the procedure and their need for proper fixation during the whole scanning process. OCT protocol included radial scans centered on the lesions (6 or 12 mm, 12 scans, 1 clock hour apart). Only high-resolution scans with good signal strength were selected. Successful OCT scans could be obtained in 13 patients and were included in the analysis.

Results

Demographics

Thirteen patients who met the above inclusion criteria were recruited in the study. The mean age of the tumor diagnosis was 3.16 ± 1.40 years and the mean age at inclusion into the study was 6.15 ± 1.95 years. Of the total 13 children recruited, 8 cases (58%) were males and 5 cases (42%) were females. The most common presentation of the tumor was leucocoria (nine cases) followed by strabismus (four cases).

Characteristics

Out of the 13 cases, 7 (53%) had bilateral tumors and 6 (47%) had unilateral tumors. Of the bilateral cases, three cases had regressed extramacular lesions in the fellow eye and four eyes had been enucleated for advanced RB in the course of treatment. Among the 13 eyes of regressed macular RB studied, 7 cases (53%) were group B tumors, 4 cases (30%) were group C tumors, and 2 cases (17%) were group D tumors. Involvement of the fovea was seen in seven eyes. All cases had received triple regimen chemotherapy (vincristine, etopside, and carboplatin). No other modality of treatment was used for these macular lesions. Regression pattern of fovea involving lesions was type 1 (four eyes), type 3 (two eyes), and type 2 (one eye). Regression pattern in non-fovea involving lesions was type 2 (two eyes), type 3 (two eyes), and type 4 (two eyes).

SS-OCT characteristics of regressed macular RB

OCT findings of regressed macular RB are summarized in Table 1. Lesion height was not assessed as the posterior extent of the lesion could not be clearly visualized in most of the cases either due to shadowing effect or scar formation. Compared with the surrounding normal retina, the regressed lesion was isodense to hyperdense in all the cases. There was no evidence of neurosensory detachment in any case.

The location of the lesion within the retina showed three recognizable patterns:

Pattern A (three eyes) – The lesion predominantly occupied the region of outer and middle retina. In these eyes, the outer retina could not be identified and inner retina was spared which appeared to drape the tumor. The inner retinal layers could be identified only in a few scans and elsewhere the differentiation of layers could not be made out. The lesion had a slight homogeneous appearance with smooth surface [Fig. 1].

Pattern B (eight eyes) – Mixed involvement (full-thickness involvement in the center and outer layers involvement in areas surrounding the central tumor). The lesion predominantly had a heterogeneous appearance with irregular surface [Fig. 2].

Pattern C (two eyes) – Complete atrophy of retinal tissue forming a depression [Fig. 3].

Partial posterior vitreous detachment over the regressed tumor was seen in three eyes. Foveal dip was clearly identified in all nonfovea involving tumors. However, foveal dip could be identified in only one eye of fovea involving tumors. Schisis or cavitary changes in variable severity were seen within the substance of the lesion in five eyes [Figs. 4 and 5].

The choroid could not be visualized in scans with dense shadowing from calcification. In scans where there was no shadowing, the choroid showed variable degree of atrophy to complete absence (sclera could be easily visualized in these scans).

Intralesion calcification of variable degree was found in eight eyes. Calcification was invariably found in scans which showed full-thickness retinal involvement. Calcification was typically absent or of lesser severity in scans which showed sparing of inner retina over the tumor and in tumors with atrophic (type 4) regression.

There was no evidence of subretinal fluid in any of the scans.

Discussion

Imaging has become an essential element in the practice of ocular oncology. It plays an important role starting from diagnosis and documentation, decision-making, and follow-up. OCT has been shown to be extremely useful for management of posterior segment disorders in children. Shields *et al.* in 2004 had demonstrated the utility of office-based time-domain OCT in children as young as 3–4 years.[16] However, with the advent of hand-held SD-OCT, its utility has been expanded to a number of clinical conditions in children. It has been shown to be useful in abusive head trauma, retinopathy of prematurity, ocular albinism, nystagmus, pediatric optic neuropathies, pediatric glaucoma, and pediatric retinal tumors.[5-7,17,18] In the field of pediatric ocular oncology, hand-held OCT has found utility in the management of tumors such as combined hamartoma of retina and retinal pigment epithelium, astrocytic hamartoma, and RB.[16,19,20] In cases of RB, hand-held SD-OCT has been useful in directing diagnosis, taking treatment decisions, monitoring tumor regression, and for follow-up.[8-12] It has also been able to detect certain clinically subtle but important findings such as detection of ophthalmoscopically invisible tumors, choroidal relapse, optic nerve head infiltration, and to know the characteristics of vitreous seeds.[8,21] Thus, OCT has been successfully added as a technological armamentarium in the management of RB. However, the use of this technology is sought with certain limitations. Hand-held device is not readily available at all centers and has a learning curve with technical difficulties in imaging. In addition, SD-OCT has limitations in imaging large tumors with limited depth of focus.[13]

In our study, we selected children who would cooperate for office-based examination. All the 13 children were co-operative for the scans. Use of SS-OCT had several advantages in our study. The scanning speed is rapid with upto 10,000 A-scans per

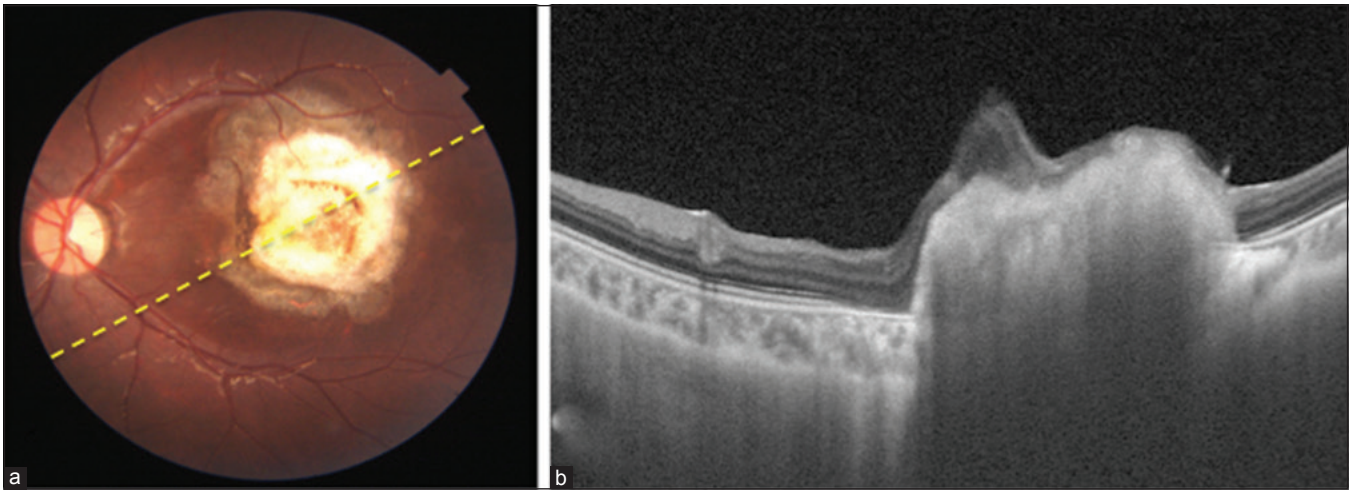

Figure 1: (a and b) Fundus picture and corresponding OCT image showing Pattern A regression. The lesion predominantly occupies the region of outer and middle retina. The outer retina cannot be identified and inner retina appeared to drape the tumor

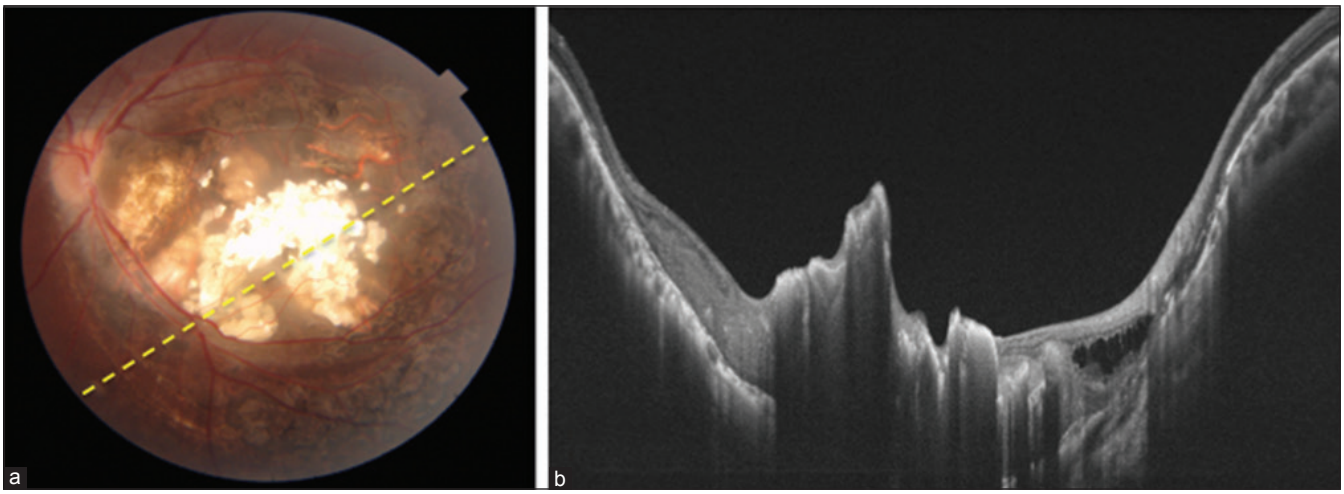

Figure 2: (a and b) Fundus picture and corresponding OCT image showing Pattern B regression. There is full-thickness involvement in center and outer layer involvement in areas surrounding the central lesion). Presence of significant calcification and schitic changes can also be noted. The lesion predominantly had a heterogeneous appearance with irregular surface

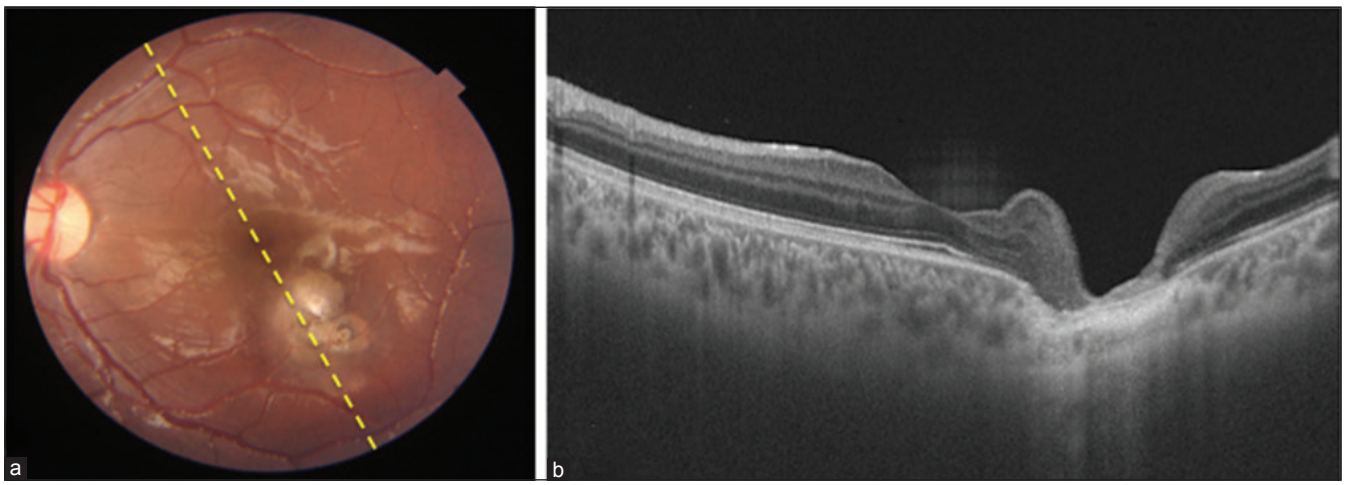

Figure 3: (a and b) Fundus picture and corresponding OCT image showing Pattern C regression. There is complete atrophy of retinal tissue at the site of regressed RB lesion forming a depression

second, hence overcomes problems related to patient fatigue. It has deep penetration, and hence there is clear visualization of the entire lesion from vitroretinal interface to the chorioscleral junction (except when there was shadowing effect). In addition, the tracking system incorporated into the system helps take multiple scans at the area of interest in children who tend to get easily distracted during the scanning session.

Of the 13 patients with macular RB, 54% had group B tumors, 31% had group C, and 15% had group D tumors. This is comparable to that reported by Pica *et al.* (group B – 47%, group C – 40%, and group E – 13%).[22] Involvement of fovea by the tumor is a major determinant of visual acuity as reported by the previous studies.[23,24] In our study, seven eyes had foveal involvement and six eyes did not have lesion involving the fovea. However, visual acuity was not documented in this study.

Studies have described the features of active RB. The OCT appearance of active RB varies with the size of lesion.

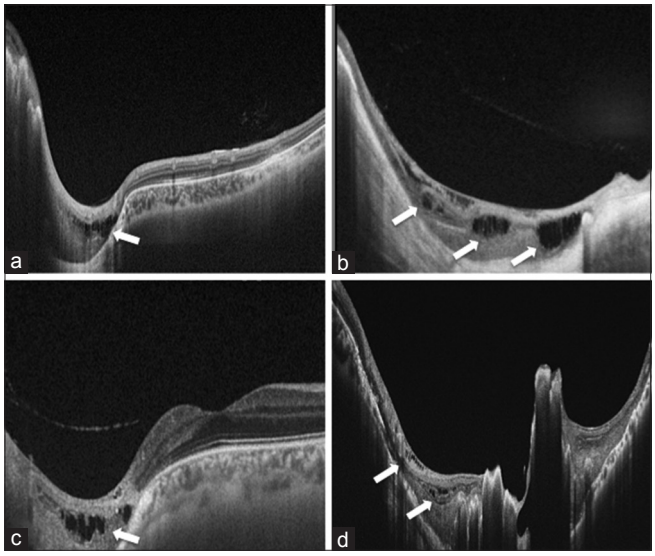

Figure 4: (a-d) SS-OCT images of various patients (number 1, 3, 10, and 12, respectively) showing schisis within the lesion (white arrows)

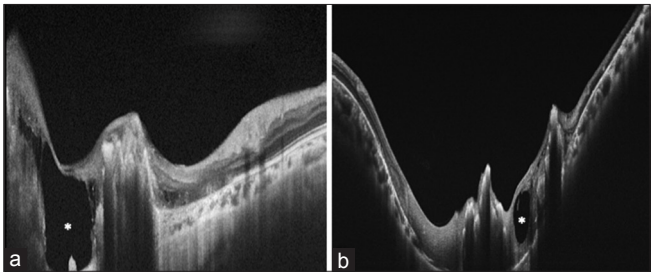

Figure 5: (a and b): SS-OCT images of patients 3 and 12 showing presence of cavitary changes (white asterisks)

Table 1: Demographic details, lesion characteristics, and swept source-OCT features of patients with macular retinoblastoma

Patient no	Age in years	Sex	Laterality	Tumour Group (Right eye Left eye)	Foveal involvement by macular tumour	Type of clinical regression	PVD over tumour	Intratumour schisis/ cavitation	OCT pattern	Foveal dip on OCT	Calcification
1	4	F	Bilateral	Macular B Enucleated	Yes	1	No	Present	B	Not recognizable	Yes (full thickness)
2	5	M	Unilateral	WNL Macular B	Yes	2	No	Absent	A	Recognizable	No
3	5	F	Bilateral	Macular D Enucleated	Yes	1	Yes	Present	B	Not recognizable	Yes (full thickness)
4	6	F	Unilateral	Macular C WNL	Yes	3	No	Absent	B	Not recognizable	Yes (full thickness)
5	10	F	Unilateral	Macular C WNL	Yes	3	No	Present	A	Not recognizable	Yes (outer layers)
6	8	M	Unilateral	Macular B WNL	No	3	No	Absent	B	Not recognizable	No
7	5	M	Unilateral	WNL Macular C	No	3	No	Absent	B	Recognizable	Yes (full thickness)
8	5	M	Bilateral	Enucleated Macular B	No	4	No	Absent	C	Recognizable	No
9	4	F	Bilateral	Macular D Extramacular C	No	2	Yes	Absent	B	Recognizable	Yes (outer layers)
10	6	M	Bilateral	Macular B Enucleated	No	2	Yes	Present	A	Recognizable	No
11	5	M	Bilateral	Extramacular B Macular B	Yes	1	No	Absent	B	Recognizable	Yes (outer layers)
12	8	M	Bilateral	Extramacular A Macular C	Yes	1	No	Present	B	Not recognizable	Yes (full thickness)
13	9	M	Unilateral	Macular B WNL	No	4	yes	Absent	C	Recognizable	No

PVD=Posterior vitreous detachment, OCT=Optical coherence tomography, WNL=Within Normal Limits

Medium-sized lesions appear as relatively homogeneous hyperdense elevations involving the middle and outer retinal layers, with shadowing of the underlying structures. Small lesions are spherical isodense lesions with a distinctive intraretinal location. The intact inner retina is usually seen to drape the tumor.[12,13] Cao *et al.* have described active RB lesions to have smooth tumor surface with low to intermediate optical density and abrupt transition from normal retina to involved retina. Normal, anatomically intact retina appeared draped over the exophytic tumor.[25]

With response to treatment, there is a sequential change from a localized, isodense intraretinal mass to a progressively more variably dense, flat, full-thickness chorioretinal scar.[13] Cao *et al.* have shown that on OCT, regressed lesions had smooth surface with high optical density with sharp transition from normal retina. The outer retina was thinned or normal and the normal retina was draped over regressed tumor.[25]

All these OCT features cannot be generalized to different patterns of regression. We noted that regressed macular RB lesions showed three distinct regression patterns on SS-OCT. The cause of this difference in appearance is not exactly known. Previous studies have shown that the variance in clinical regression patterns could be due to the difference in initial tumor size, degree of tumor differentiation, mode of therapy, and distance from fovea. Similarly, in our series, we found that small lesions away from fovea had OCT pattern C and larger lesions had either pattern A or B.

Other features that were documented include partial posterior vitreous detachment noted in three eyes and intralesion calcification of variable degree in eight eyes. It is of interest to note that calcification was not detectable even on OCT in the remaining five eyes. In addition, schisis/cavitary changes were noted in five eyes. The appearance of schisis in RB is probably due to intact Muller cells bridging degenerated retinal layers with underlying varying degree of sclerochoroidal atrophy or excavation. Cavitary changes that were not seen clinically were detected on OCT in two patients. The presence of cavitary changes within the tumor have been speculated to be an indicator of a more differentiated tumor.[26]

There are a few limitations in the study. We studied only older children (4 years and above) as the SS-OCT in its current version is only available for office use. Future developments may allow the use of this technology in both operation theaters and in offices. Also, this study included only cases of regressed RB. It would be ideal to do a prospective study to include cases of active RB and follow-up them with OCT scans as is done with other disorders of the retina. Also, the study is limited by a small number of study patients.

Conclusion

SS-OCT was useful to image cases of regressed RB including large lesions and provided insight into the understanding of the various OCT-based regression patterns of RB. Rapid scan acquisition time and tracking facility with SS-OCT system helped in successful imaging even in smaller children.

Compliance with ethical standards

Institute ethics committee clearance was taken prior to the beginning of study and all procedures performed in this study were done in accordance with the ethical standards of the institutional ethics committee and adhered to the tenets of Declaration of Helsinki.

Informed consent

Appropriate written informed consent has been obtained from the parents of all patients.

Financial support and sponsorship

Nil.

Conflicts of interest

There are no conflicts of interest.

References

1. Shields JA, Shields CL. Intraocular Tumors – A Text and Atlas. Philadelphia, PA, USA: WB Saunders Company; 1992.
2. Dimaras H, Kimani K, Dimba EA, Gronsdahl P, White A, Chan HS, *et al*. Retinoblastoma. Lancet Lond Engl 2012;379:1436-46.
3. Tamboli A, Podgor MJ, Horm JW. The incidence of retinoblastoma in the United States: 1974 through 1985. Arch Ophthalmol Chic Ill 1960 1990;108:128-32.
4. Sanders BM, Draper GJ, Kingston JE. Retinoblastoma in Great Britain 1969-80: Incidence, treatment, and survival. Br J Ophthalmol 1988;72:576-83.
5. Stathopoulos C, Gaillard MC, Puccinelli F, Maeder P, Hadjistilianou D, Beck-Popovic M, *et al*. Successful conservative treatment of massive choroidal relapse in 2 retinoblastoma patients monitored by ultrasound biomicroscopy and/or spectral domain optic coherence tomography. Ophthalmic Genet 2018;39:242-6.
6. Muni RH, Kohly RP, Sohn EH, Lee TC. Hand-held spectral domain optical coherence tomography finding in shaken-baby syndrome. Retina Phila Pa 2010;30(4 Suppl):S45-50.
7. Chavala SH, Farsiu S, Maldonado R, Wallace DK, Freedman SF, Toth CA. Insights into advanced retinopathy of prematurity using handheld spectral domain optical coherence tomography imaging. Ophthalmology 2009;116:2448-56.
8. Chong GT, Farsiu S, Freedman SF, Sarin N, Koreishi AF, Izatt JA, *et al*. Abnormal foveal morphology in ocular albinism imaged with spectral-domain optical coherence tomography. Arch Ophthalmol Chic Ill 1960 2009;127:37-44.
9. Soliman SE, VandenHoven C, MacKeen LD, Héon E, Gallie BL. Optical coherence tomography-guided decisions in retinoblastoma management. Ophthalmology 2017;124:859-72.
10. Lee H, Proudlock FA, Gottlob I. Pediatric optical coherence tomography in clinical practice – Recent progress. Invest Ophthalmol Vis Sci 2016;57:OCT69-79.
11. Seider MI, Grewal DS, Mruthyunjaya P. Portable optical coherence tomography detection or confirmation of ophthalmoscopically invisible or indeterminate active retinoblastoma. Ophthalmic Surg Lasers Imaging Retina 2016;47:965-8.
12. Berry JL, Cobrinik D, Kim JW. Detection and intraretinal localization of an "invisible" retinoblastoma using optical coherence tomography. Ocul Oncol Pathol 2016;2:148-52.
13. Rootman DB, Gonzalez E, Mallipatna A, Vandenhoven C, Hampton L, Dimaras H, *et al*. Hand-held high-resolution spectral domain optical coherence tomography in retinoblastoma: Clinical and morphologic considerations. Br J Ophthalmol 2013;97:59-65.
14. Shields CL, Mashayekhi A, Cater J, Shelil A, Ness S, Meadows AT, *et al*. Macular retinoblastoma managed with chemoreduction: Analysis of tumor control with or without adjuvant thermotherapy in 68 tumors. Arch Ophthalmol Chic Ill 1960 2005;123:765-73.
15. Shields CL, Palamar M, Sharma P, Ramasubramanian A, Leahey A,

Meadows AT, *et al*. Retinoblastoma regression patterns following chemoreduction and adjuvant therapy in 557 tumors. Arch Ophthalmol Chic Ill 1960 2009;127:282-90.

16. Shields CL, Mashayekhi A, Luo CK, Materin MA, Shields JA. Optical coherence tomography in children: Analysis of 44 eyes with intraocular tumors and simulating conditions. J Pediatr Ophthalmol Strabismus 2004;41:338-44.
17. Ghasia FF, Freedman SF, Rajani A, Holgado S, Asrani S, El-Dairi M. Optical coherence tomography in paediatric glaucoma: Time domain versus spectral domain. Br J Ophthalmol 2013;97:837-42.
18. Gospe SM, Bhatti MT, El-Dairi MA. Emerging applications of optical coherence tomography in pediatric optic neuropathies. Semin Pediatr Neurol 2017;24:135-42.
19. Mallipatna A, Vinekar A, Jayadev C, Dabir S, Sivakumar M, Krishnan N, *et al*. The use of handheld spectral domain optical coherence tomography in pediatric ophthalmology practice: Our experience of 975 infants and children. Indian J Ophthalmol 2015;63:586-93.
20. Shields CL, Manalac J, Das C, Saktanasate J, Shields JA. Review of spectral domain-enhanced depth imaging optical coherence tomography of tumors of the retina and retinal pigment epithelium in children and adults. Indian J Ophthalmol 2015;63:128-32.
21. Berry JL, Anulao K, Kim JW. Optical coherence tomography imaging of a large spherical seed in retinoblastoma. Ophthalmology 2017;124:1208.
22. Pica A, Moeckli R, Balmer A, Beck-Popovic M, Chollet-Rivier M, Do HP, *et al*. Preliminary experience in treatment of papillary and macular retinoblastoma: Evaluation of local control and local complications after treatment with linear accelerator-based stereotactic radiotherapy with micromultileaf collimator as second-line or salvage treatment after chemotherapy. Int J Radiat Oncol Biol Phys 2011;81:1380-6.
23. Kim JM, Kim JH, Kim SJ, Park KD, Shin HY, Ahn HS, *et al*. Visual prognosis of retinoblastoma in the posterior pole treated with primary chemotherapy plus local treatments. Korean J Ophthalmol 2010;24:347-52.
24. Weiss AH, Karr DJ, Kalina RE, Lindsley KL, Pendergrass TW. Visual outcomes of macular retinoblastoma after external beam radiation therapy. Ophthalmology 1994;101:1244-9.
25. Cao C, Markovitz M, Ferenczy S, Shields CL. Hand-held spectral-domain optical coherence tomography of small macular retinoblastoma in infants before and after chemotherapy. J Pediatr Ophthalmol Strabismus 2014;51:230-4.
26. Mashayekhi A, Shields CL, Eagle RC, Shields JA. Cavitary changes in retinoblastoma: Relationship to chemoresistance. Ophthalmology 2005;112:1145-50.